



Comparison between thermal sampling and numerical analysis of thermally stimulated depolarization current peaks

E. Laredo, A. Bello, M. C. Hernández, and M. Grimau

Citation: [Journal of Applied Physics](#) **90**, 5721 (2001); doi: 10.1063/1.1413707

View online: <http://dx.doi.org/10.1063/1.1413707>

View Table of Contents: <http://scitation.aip.org/content/aip/journal/jap/90/11?ver=pdfcov>

Published by the [AIP Publishing](#)



Re-register for Table of Content Alerts

Create a profile.



Sign up today!



Comparison between thermal sampling and numerical analysis of thermally stimulated depolarization current peaks

E. Laredo,^{a)} A. Bello, and M. C. Hernández

Department of Physics, Universidad Simón Bolívar, Apartado 89000, Caracas 1080, Venezuela

M. Grimau

Department of Materials Science, Universidad Simón Bolívar, Apartado 89000, Caracas 1080, Venezuela

(Received 1 May 2001; accepted for publication 28 August 2001)

Thermal sampling peaks recorded after windowing polarization are studied for the segmental mode in poly(ϵ -caprolactone). Also, numerical decompositions of the global thermally stimulated depolarization current peak into pure Debye contributions are performed with direct signal analysis (DSA) and simulated annealing direct signal analysis procedures for Arrhenius and Vogel–Tammann–Fulcher (VTF) temperature dependences, respectively. It is found that the results between the experimental and the numerical procedures agree very well and the approximations made in the analysis of the experimental curves are thus validated, despite the unphysical values for the relaxation parameters found by both methods when using Arrhenius relaxation times. On the contrary, when VTF relaxation times are used for the numerical decomposition, agreement is found with the results of isothermal dielectric absorption as a function of frequency, together with reasonable values for reorientation energies, pre-exponential factors and VTF temperature. Thermal sampling and DSA also compare well when studying the departure from the zero-entropy line which indicates the onset of a cooperative character in the dynamics of molecular motion. Compensation is found whenever the primary relaxation is analyzed with Arrhenius or Eyring relaxation times and does not appear when VTF relaxation times are used in the numerical decomposition. © 2001 American Institute of Physics. [DOI: 10.1063/1.1413707]

I. INTRODUCTION

Thermally stimulated depolarization current (TSDC) techniques have been widely used for the detailed study of the relaxation processes in polymeric materials with dipolar molecular segments present in their structure. The TSDC technique is equivalent to dynamic dielectric spectroscopy performed as a function of temperature at an equivalent frequency in the mHz range. The resolution is thus very high and besides, the overlapping modes, which are a feature of the dielectric spectrum of these complex materials, can be isolated by carefully selecting the polarization conditions. The chosen polarization temperature, T_p , determines the dipoles that will orient under the action of the applied electric field, E_p , during the polarization step; the dipolar segments that at this temperature have a longer relaxation time as compared to the polarization time, will not contribute to the polarization frozen in during the following cooling step. Moreover, by proceeding to a partial depolarization of the low temperature tail of a TSDC peak, i.e., cooling down the sample after the dipoles with shorter relaxation times are randomized, a “clean peak” is obtained on a subsequent heating. This capability of the technique has opened a wide range of variations, the most used one being the thermal sampling (TS) procedure¹ which is an attempt to isolate experimentally each of the elementary (Debye) relaxation processes whose sum causes the TSDC global spectrum. In this way, as each of the isolated peaks is assumed to be charac-

terized by a single relaxation time, $\tau_i(T)$, the distribution of relaxation times of the elementary contributions is obtained. Global TSDC, TS, and peak cleaning techniques have been successfully applied in polymers to the study of the dielectric manifestation of the segmental motions occurring at the glass transition temperature, α mode,² and to the secondary relaxations, labeled β and γ modes,³ which occur at lower temperatures and are attributed to more localized motions of segments of variable but shorter lengths. Above the glass transition temperature, the observed TSDC peaks are related to the displacement of free charges in the sample⁴ and being very intense sometimes renders the detection of neighboring dipolar modes difficult.

The analysis of the peaks, isolated experimentally by the TS technique, is based on the assumption of a Debye character, which is not often the case, and on some approximations introduced in the ulterior calculations.⁵ Instead of the TS, the decomposition of the global TSDC peak into true Debye peaks can be attempted by numerical methods. The direct signal analysis (DSA)⁶ and the simulated annealing direct signal analysis (SADSA)⁷ computer procedures have been proposed as an alternative to the experimental determination of the relaxation time distribution. The advantage of the numerical methods applied to TSDC global peaks is that the decomposition in Debye peaks is performed without any approximation and the relaxation time, together with the precise contribution to the total polarization of each elementary process, are precisely calculated. The results of the adjustment procedure of the TSDC peak are remarkably

^{a)}Electronic mail: elaredo@usb.ve

good as the sum of squared residuals can be as low as 10^{-9} for a current density peak whose area is normalized to a unit polarization.

Once the TS decomposition is performed, the relaxation time variation with temperature can be estimated in each case. $\tau_i(T)$ is calculated following the Bucci, Fieschi, and Guidi (BFG) area method.⁸ Assuming Arrhenius relaxation times for each elementary peak

$$\tau_i(T) = \tau_{0i} \exp(E_{ai}/kT), \quad (1)$$

where the activation energy, E_{ai} and the pre-exponential factor, τ_{0i} , characteristic of each process are calculated from the slope and the intercept of the $\log(\tau_i)$ vs $1/T$ plot. It is often found that there exists a linear relationship among $\log(\tau_{0i})$ and the reorientation energies, E_{ai} , determined from the decomposition of the global TSDC peak. This is reported in the literature as a compensation law⁹ and has been found for both the secondary¹⁰ and the α modes in a wide variety of amorphous or semicrystalline polymers.¹¹ This effect can also be visualized as a convergence to a single point of all the extrapolated lines in the Arrhenius plot $\log(\tau_i)$ vs $1/T$. The existence of a compensation point implies that there exists a temperature T_C at which all the elementary modes relax with an identical relaxation time, τ_c . Compensation has been often interpreted as an indication of a common origin for the elementary processes which follow the rule and to the existence of cooperative motions at the origin of the global relaxation process decomposed by the TS technique.⁵ This interpretation is controversial and the extremely low values found for the pre-exponential factors which can reach 10^{-50} s, together with the high reorientation Arrhenius energies (several electron volts) are beyond any physical significance. The absence of meaning of compensation has been alternatively attributed to a variety of causes such as the propagation of experimental errors,¹² the fact that the activation energy and activation entropy are not independent,¹³ or a result of the mathematical manipulation of the equations in an underdetermined system.⁹ Consequently, compensation can not be related to any material property as it has been argued. Alegria *et al.*¹⁴ even conclude that the compensation law in the α relaxation range is an artifact and that the TSDC experiments can not discriminate among heterogeneous (relaxation time distribution) and homogeneous scenarios.

An alternative analysis has been proposed by Starkweather¹⁵ based on the distinctive behavior of the Arrhenius (or Eyring) relaxation parameters of local and cooperative modes. The activation energy of the elementary peaks obtained from the TS of secondary relaxations, in the absence of any cooperative character, should vary as a function of the polarization temperature following a zero entropy line, while those derived from the decomposition of the segmental mode should deviate from this line and show a steep energy increase. This approach has been successfully applied to poly(methylmethacrylate),¹⁶ fluoropolymers,² and thermoplastics polyesters.¹¹

Another point to be noted on these thermally activated techniques is the problem of a possible evolution of the material and the dynamics of the motion one wants to determine due to the physical aging of the polymer as we move towards

the glass transition temperature. If the thermal history is the same, the results can be easily compared and care should be taken to ensure this requisite. The usual temperature program in a TS experiment keeps a constant polarization time and the sample is short circuited for a constant time after the field is switched off at a temperature $T_p - \Delta T$ ($\Delta T \leq 5$ K). As the polarization temperature is increased, the structural recovering process will occur with a higher efficiency due to the increased chain mobility. Alegria *et al.*¹⁴ have proposed a somewhat different experimental protocol for TS experiments which allows one to keep the thermal history of the sample independent of the polarization temperature.

In this work, we have performed both TS experiments and numerical decompositions using DSA and SADSA procedures in order to compare the results obtained with these two different approaches for determining the relaxation time distribution, thus evaluating the validity of the assumptions and approximations made in the analysis of the TS results. It is not the aim of this work to discuss the physical meaning of compensation based on the assumption of Arrhenius relaxation times in the whole temperature range covered by secondary and primary relaxations, which is always used in the analysis of the TS curves. The numerical analysis of a global TSDC peak by using Vogel–Tammann–Fulcher (VTF) relaxation times is the best approximation to the extraction of the relaxation time distribution of the α mode. The material chosen is the semicrystalline poly(ϵ -caprolactone) (PCL) and the relaxation studied is the primary relaxation which occurs at 210 K. The detailed study of the chain motion in this homopolymer is important so as to compare it with the behavior observed when PCL is used as a component of triblock copolymers (with polystyrene and polybutadiene) where the segregation might have an effect on the time scale of the dielectric relaxations.

II. THEORY

The standard way to analyze TS peaks is based on the BFG area method⁸ for the current density, $J_i(T)$, recorded for a Debye TSDC peak and its relationship with the relaxation time

$$J_i(T) = \frac{P_i(T)}{\tau_i(T)}, \quad (2)$$

where $P_i(T)$ is the residual polarization and $\tau_i(T)$ the relaxation time at each temperature T . The residual polarization is easily determined from the area under the TSDC elementary peak from T to the end of the high temperature tail of the curve, $J_i(T)$ being the ordinate of the curve at this same temperature. The relaxation times calculated from part of the rise of each elementary peak analyzed in this way are represented in an Arrhenius plot of the relaxation times, $\log(\tau_i)$ vs $1/T$, by a line whose slope and intercept allows the calculation of the activation energy and the pre-exponential factor of Eq. (1).

In Eyring's theory of absolute reaction rates,¹⁷ the relaxation time can be written in function of the activation enthalpy, ΔH_i^* and entropy, ΔS_i^* , as

$$\tau_i(T) = \frac{h}{kT} \exp\left(-\frac{\Delta S_i^*}{k} + \frac{\Delta H_i^*}{kT}\right), \quad (3)$$

where h and k are the Planck and the Boltzmann constants, respectively. The activation entropy ΔS_i^* is related to the fraction of available sites when comparing activated states to the inactivated ones, ΔH_i^* is directly related to the height of the potential barrier to be overcome by the reorienting entity. At the temperature of the maximum, T_{mi} of each elementary peak recorded in a TS experiment, an equivalent frequency can be defined by

$$f_{mi} = \frac{1}{2\pi\tau(T_{mi})} = \frac{E_{ai}b}{2\pi kT_{mi}^2}, \quad (4)$$

where b is the constant heating rate at which the polarized sample undergoes its thermally stimulated depolarization. The activation Gibbs energy can then be written as

$$\begin{aligned} \Delta G_i^* &= \Delta H_i^* - T_{mi}\Delta S_i^* = kT_{mi}[21.922 + \ln(T_{mi}/f_{mi})] \\ &= \alpha T_{mi}, \end{aligned} \quad (5)$$

on the whole temperature range. Moura *et al.*⁹ have shown the existence of the linear dependence of ΔG_i^* on the temperature of the peak maximum for a variety of TS experiments performed on different polymeric materials. This kind of universal behavior is attributed to the lack of variation observed for the quantity between the brackets in Eq. (5) for the 960 TS experiments plotted by them performed on polymers with different chemical structures and for relaxations due to different origins (see Fig. 1 in Ref. 9). This observed general behavior can also be expressed as a liner relationship among the activation entropy and $\Delta H_i^*/T_{mi}$ and written as

$$\Delta S_i^* = \frac{\Delta H_i^*}{T_{mi}} - \alpha, \quad (6)$$

with a slope equal to 1 and an intercept $\alpha = 2.88 \times 10^{-3}$ eV K^{-1} , independently of the origin of the relaxation processes considered, its characteristics or even the chemical structure of the material under study. ΔS_i^* values can be estimated from the experimentally determined τ_{0i} and E_{ai} assuming that $\Delta H_i^* \approx E_{ai}$,

$$\Delta S_i^* = -k \left[\ln\left(\frac{kT_{mi}}{h}\right) + \ln(\tau_{0i}) \right]. \quad (7)$$

Compensation can be visualized in different ways. In the relaxation times Arrhenius plot, compensation is shown by convergence of the extrapolated straight lines representing each TS peak to a compensation point $[1/T_C, \log(\tau_c)]$ implying that at this compensation temperature, all the processes would relax with the same characteristic time. Then, the pre-exponential factors variation with the activation energies would be

$$\tau_{0i} = \tau_c \exp(-E_{ai}/kT_C). \quad (8)$$

Thus, compensation is believed to exist when a linear relationship is observed in a plot $\log(\tau_{0i})$ vs E_{ai} , drawn after the determination of the Arrhenius relaxation parameters extracted from the TS experiments. In the Eyring for-

malism compensation phenomena implies a linear relationship between ΔS_i^* and E_{ai} which is lately the most used representation. The slope of the latter line is $1/T_C$ and the intercept is $k \ln(h/k\tau_c T_C)$. The compensation parameters are characteristic of each global relaxation process observed in a given material. As opposed to the universality of the dependence described by Eq. (6), elementary processes related by compensation have been attributed to a common origin and often considered as indicative of cooperative molecular motions of dipolar segments whose length is varying. However, the existence of compensation processes for the secondary noncooperative relaxations originated by the local motion of polar side groups has often been reported.^{3,10} Compensation also exists when the Arrhenius activation energy starts to increase drastically as one approaches the glass transition temperature from the low temperature side. The values found in this zone, when using Arrhenius dependence for the relaxation times, are in the range of several eV, and consequently, the corresponding pre-exponential factors decreases in an unrealistic way reaching values of 10^{-60} s as the value of $\tau(T_{mi})$ for the usual heating rates is around 32 s. When plotting the variation of E_{ai} vs T_{Pi} or alternatively T_{mi} , it is very useful to draw the zero-entropy line, $\Delta S_i^* = 0$, which is very often calculated² assuming $f_{mi} = 5$ mHz from

$$E_{ai} = kT_{mi}[1 + \ln(kT_{mi}/h2\pi f_{mi})]. \quad (9)$$

The variation of the Eyring activation energy, $\Delta H_i^*(T_{mi})$, when $\Delta S_i^* = 0$ is found from the numerical solution of the following equation:

$$\frac{kT_{mi}^2}{b(\Delta H_i^* + kT_{mi})} = \frac{h}{kT_{mi}} \exp(\Delta H_i^*/kT_{mi}), \quad (10)$$

where the resulting line depends only on the heating rate, b .

In numerous previous works on TS on different types of polymers, it has been reported that most often the points, E_{ai} vs T_{mi} , corresponding to elementary contributions from secondary or local relaxations, follow the zero-entropy line showing the absence of cooperativity,¹¹ and start to strongly deviate from it as the temperature moves into the α region. In polymers slightly negative entropies are often reported,^{2,9,11,15} i.e., experimental points from the γ or β region which, in the E_{ai} vs T_{mi} plot, fall below the zero-entropy line described by Eq. (9).

It is widely accepted¹⁸ that for the segmental modes in polymers, the temperature dependence of the relaxation time is well described by the VTF equation

$$\tau'_i(T) = \tau'_{0i} \exp\left(\frac{E'_i}{k(T-T_0)}\right) = \tau'_{0i} \exp\left(\frac{B_i}{T-T_0}\right), \quad (11)$$

where T_0 is the ideal glass transition or Vogel temperature; below T_0 , all molecular motions are frozen. T_0 is usually found to be from 30 to 70 K below the glass transition temperature as determined by differential scanning calorimetry or the maximum of the α TSDC peak. The closer T_0 is to T_g , the more fragile the glass forming system becomes. The Williams-Landel-Ferry expression for the relaxation times is completely equivalent to the VTF equation and it has been justified by several models which include the cooperative

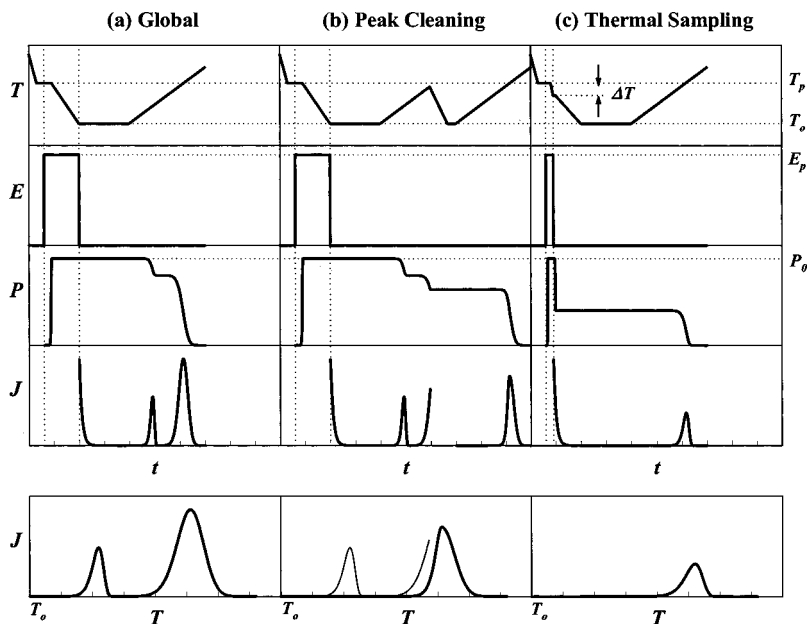


FIG. 1. Schematic of global TSDC (a), peak cleaning (b), and TS (c) techniques showing the variation with time of the temperature, T , the applied field, E_p , the polarization, P , and the depolarization current density, J . In the boxes on the last row, the lines represent $J(T)$ recorded from the initial to the final temperature of the experiment.

character of the α relaxation such as the free volume point of view¹⁹ or the molecular kinetic theory²⁰ based on the variation with temperature in the size of the cooperatively rearranging regions in glass forming liquids.

III. EXPERIMENTS AND COMPUTER ANALYSIS

A. Experimental

In order to compare the TS and the DSA analysis results, TSDC experiments are performed on compression molded films of PCL with an average thickness of 359 μm . The crystallinity degree of our samples is 64% as measured by wide-angle x-ray diffraction at room temperature. The PCL used (Aldrich Chemicals), has a number-average molecular weight $\bar{M}_n = 100\,000$ g/mol and a polydispersity of 1.56 measured by Gel Permeation Chromatography. The TSDC PCL samples are disk shaped 20 mm in diameter.

The experimental setup used to perform the TSDC characterization has been designed in our laboratory.²¹ The polarization step is performed in a nitrogen atmosphere, the cell being thoroughly evacuated to avoid any moisture trace. At the depolarization stage, the sample is heated at a constant rate of 0.07 K/s in a helium atmosphere of 150 Torr from 80 K to above the polarization temperature, T_p . The temperature control system allows one to regulate the depolarization process at a constant heating rate that induces the TSDC current measured with a Keithley 642 electrometer connected in series to the measuring cell where the sample is located between two metallic electrodes.

The TSDC characterizations can be differentiated by three types of polarization protocols whose sequence is shown in Fig. 1. In the first polarization protocol, Fig. 1(a) the electric field is applied during a time t_p (typically 3 min) at a polarization temperature T_p , and during the cooling of the sample to 80 K; the global TSDC peak is recorded as the temperature increases at a linear rate. A “clean” peak is obtained when the sample is discharged by heating to a temperature from 10 to 30 K below the maximum of the peak,

T_m , as shown in Fig. 1(b). Then the sample is quenched again to low temperatures before recording the “clean” TSDC spectrum as the temperature is raised at a constant rate. This particular protocol allows the isolation of the α relaxation from the secondary processes thermally activated at lower temperatures.

The TS polarization protocol starts with an identical polarization step at T_p , Fig. 1(c); then the sample is cooled at a rate of 0.056 K/s until a temperature $T_p - 5$ K, where the electric field is turned off. The sample is maintained at this temperature for 1 min and then quenched to 80 K. It is assumed that the TS spectrum obtained is originated by a single Debye process, and is characterized by single values for the activation energy and pre-exponential factor. The global TSDC peak is the composition of these elementary peaks that can be isolated by TS. This polarization protocol is repeated at different polarization temperatures at intervals of 5 K in the temperature range covered by the global peak. The first polarization protocol is used here to generate the spectra studied by the DSA numerical decomposition and the third one is applied in order to compare the DSA and TS results. The clean curves obtained with the second polarization program are analyzed with the DSA or SADS computer procedures.

B. DSA and SADS procedures

DSA has been described in detail and has been applied to the decomposition of relaxations in several polymers;⁶ it is a numerical decomposition of the global TSDC spectra in M elementary Debye peaks each of them characterized by a single Arrhenius relaxation time, E_{ai} and τ_{0i} , and its contribution to the total polarization is P_{0i} . The computer program uses the nonlinear least squares fitting procedure to adjust the M energy bins chosen in an energy window. The output of the program is the M values of E_{ai} , τ_{0i} , P_{0i} , and the corresponding T_{mi} is calculated from the E_{ai} and τ_{0i} values. The sum of squares residuals is always very low ($< 10^{-8}$ for a

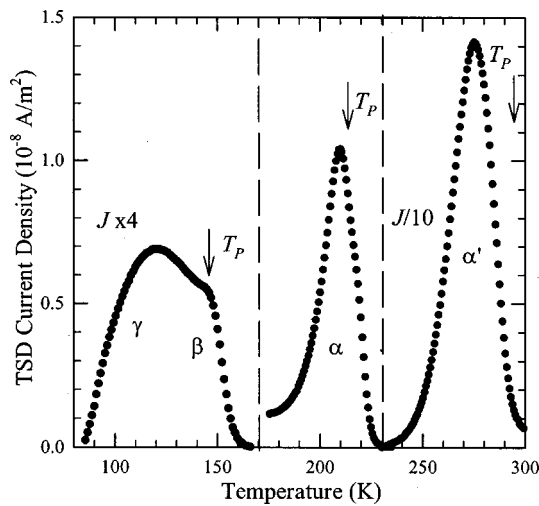


FIG. 2. TSDC global spectrum of PCL $M_n = 100\,000$ g/mol. The left-hand side scale corresponds to the α relaxation. This scale is divided by 4 for the γ and β relaxation and multiplied by 10 for the α' relaxation. The polarization temperatures are indicated by arrows.

TSDC curve with a unit polarization). A significant improvement to the DSA is the SADS procedure^{7,22} which uses a Monte Carlo algorithm and has the advantage of converging, independently of the starting values given to the adjustable parameters, to the global minimum of the function to be minimized if the simulated annealing of the system is carried on with a schedule which guarantees the reach of equilibrium at each “temperature” step. The SADS has been used here to analyze the segmental relaxation when the VTF temperature dependence for the relaxation time of each elementary mode is used.

IV. RESULTS AND DISCUSSION

In Fig. 2, the global TSDC spectrum of PCL is shown, with three very clearly defined relaxation regions. The lowest temperature region corresponds to the weak secondary relaxations, labeled γ and β , attributed to the restricted motions of short segments with dipolar moments. This broad peak is clearly a multicomponent relaxation and a distribution of relaxation times must be sought in order to describe the experimental profile in an heterogeneous scenario. The dielectric manifestation of the glass transition is the α mode which is narrow and located at $T_g \sim T_{m\alpha} = 210$ K which is six times more intense than the secondary relaxations. At still higher temperatures, an α' peak exists which has been studied in detail and its origin attributed to an interfacial polarization in this semicrystalline polymer.⁴ The global TSDC dipolar relaxations of PCL have been analyzed with DSA (γ , β , α peaks) and SADS (α peak) and the results of the numerical decompositions in elementary modes either with Arrhenius or VTF relaxation times are given respectively, in terms of the activation energy and pre-exponential factors for each i th elementary mode of the set of M modes which best describe the distribution, each with a contribution P_{0i} . In this section a detailed comparison of the results obtained by applying the TS technique and the DSA procedure to the α mode in PCL, which is originated by the dipolar motions that occur at the

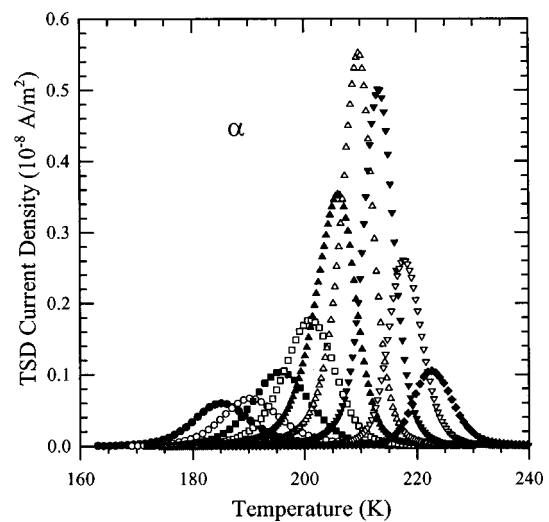


FIG. 3. TS curves from the glass transition mode of PCL. The polarization temperatures varied from the left- to the right-hand side from 180 (●) to 220 K (◆) by 5 K steps, the polarization window is $\Delta T = 5$ K, the external field is $E_p = 0.557$ MV/m the heating rate is $b = 0.07$ Ks⁻¹.

glass transition, are presented. In Fig. 3, the current density of the TS peaks is plotted as a function of temperature; the polarization temperatures range from 180 to 220 K and the polarization window is $\Delta T = 5$ K, in order to compare our results with the most frequently used temperature program just described. Each elementary peak is then analyzed with the BFG method⁸ to find the variation of $\tau_i(T)$, Eq. (2). Due to the impossibility to isolate a single Debye peak in a TS nonisothermal scan, the most commonly used procedure to calculate $\tau_i(T)$ consists in considering only part of the rise of the current density curve where a linear relationship between $\log(\tau_i)$ vs $1/T$ is observed. To approximate the residual polarization at each temperature, $P_i(T)$, instead of evaluating the area under the TS curve for temperatures higher than the current temperature, the residual polarization corresponding to the decay of the current density, $T \geq T_m$, is approximated by its expected fraction of the total polarization,⁵ P_0 ; this in turn is estimated from the area under the curve from the initial temperature to T_m by $P_0 = (1.6245/b) \int_{T_i}^{T_m} J(T) dT$. In this way, the decay of the TS curve is discarded and replaced by the area it should have if only the relaxation time determined with the rise of the curve exists. This approximation is done to correct the situation stemming from the impossibility of isolating a unique Debye peak when using the TS technique. Following this procedure to calculate the relaxation times as a function of temperature for each elementary peak, the Arrhenius plot in Fig. 4 shows the results obtained. Even with the approximations made, one can only use a narrow temperature range over which the linear relationship among $\log(\tau_i)$ vs $(1/T)$ can be drawn, i.e., the rise of the depolarization current, and it roughly covers relaxation times over two decades. This is a common feature in TS results¹⁶ where the useable zone in the experimental curves $\tau(1/T)$ has to be carefully selected. The assumption made to estimate P_0 from the area under the rise of the current peak might be a matter of discussion if even the low temperature side of the peak is not accurately described by a single relaxation time. The set

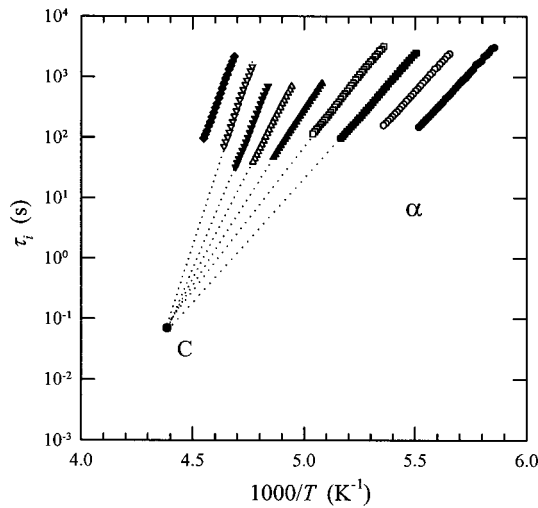


FIG. 4. Relaxation plot $\tau_i(1/T)$ obtained from TS of the α mode of PCL. The polarization temperature decreases from 220 to 180 K by 5 K steps on going from the left- to the right-hand side. The compensation point C is obtained from the plot in Fig. 5, $\tau_c=0.07$ s and $T_C=229$ K.

of points, $\log(\tau_i)$ vs $(1/T)$ corresponding to the rise of the i th TS peak is then adjusted to an Arrhenius law whose slope is the activation energy, E_{ai} , and intercept the pre-exponential factor, $\log(\tau_{0i})$. The energies found here vary between 0.8 and 2.1 eV and the corresponding pre-exponential factors range from 10^{-20} to 10^{-50} s which are far too out of scale to deserve any sound explanation. A similar analysis can be performed to determine the Eyring parameters ΔH_i^* and ΔS_i^* by plotting $\tau_i T$ vs $1/T$ and determining the slope and the intercept of the line drawn in the (limited) range where a linear relationship is observed. The activation enthalpies and entropies range from 0.8 eV to 2.1 eV and from 0.001 eV u^{-1} to 0.007 eV K^{-1} , respectively.

TS results are generally presented^{1,3,5,14,16} on a $\log(\tau_{0i})$ as a function of E_{ai} plot, as shown in Fig. 5. The TS peaks are analyzed with Arrhenius relaxation times (empty circles, right-hand vertical axis) or with Eyring relaxation times (filled circles, left-hand side vertical axis). The linear dependence found either on the $\log(\tau_{0i})$ vs E_{ai} or on ΔS_i^* vs ΔH_i^* plot, might be interpreted as the existence of compensation with a compensation time τ_c and compensation temperature T_C

$$\tau_{0i} = \tau_c \exp\left(\frac{E_{ai}}{kT_C}\right), \quad \Delta S_i^* = k \ln\left(\frac{h}{k\tau_c T_C}\right) + \frac{\Delta H_i^*}{T_C}. \quad (12)$$

The compensation point obtained from the TS data only, analyzed with Arrhenius or Eyring dependences, is $\tau_c = (0.07 \pm 0.06)$ s, $T_C = (229 \pm 2)$ K which is plotted in Fig. 4 as point C. Following Dargent *et al.*,¹¹ the dotted lines which converge reasonably well here to point C are extrapolations of the Arrhenius lines determined by the experimental points only. Often, the dashed lines are forced through the compensation point determined from the linear relationship of $\log(\tau_{0i})$ vs E_{0i} and differ from the extrapolated lines defined by the experimental points only.

A curvature is often observed in these relaxation plots as the temperature of the maximum of the TS peak approaches

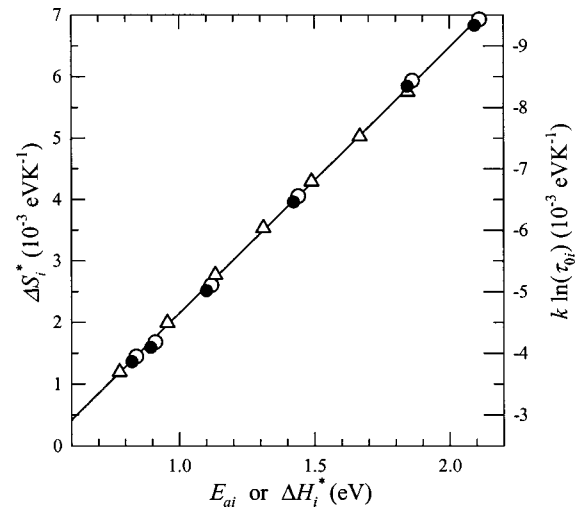


FIG. 5. Compensation curve: ● TS calculated with Eyring formalism, left-hand side vertical axis increasing upwards, $\Delta S_i^* = f(\Delta H_i^*)$; ○ TS calculated with Arrhenius relaxation times, right-hand side vertical axis increasing downwards $k \ln(\tau_{0i}) = f(E_{ai})$. The compensation point from TS is $\tau_c = 0.07$ s, $T_C = 229$ K. Δ corresponds to the DSA results in Fig. 6, right-hand side vertical axis. The compensation point from DSA is $\tau_c = 0.009$ s and $T_C = 234$ K. The continuous line is the best fit to all the points.

or is larger than T_g , even if a reduced temperature interval is considered, and it has been often attributed²³ to the difficulty found in isolating a pure Debye peak in spite of the narrow polarization windows commonly used. This argument is not very convincing as with the approximations made in the usual framework, one should be able to isolate a nearly single Debye peak. If $P(T_m)$, the polarization remaining at $T = T_m$, is not measured from the corresponding area under the TS curve for $T \geq T_m$, but calculated from the fraction of the total polarization it should have if the TS peak was purely Debye, the broadening effect of the TS peak should be negligible. Moreover, the curvature should also be observed in the TS of secondary or noncooperative relaxation peaks as the distribution found there is wide and the isolation of a single peak by TS should be equally difficult. As in the relaxation plots which show compensation for secondary relaxations,^{3,10,24} this is not the case, it appears that this argument which should also be valid for the β mode is not justified.

The global TSDC peak corresponding to the α mode of PCL is now analyzed by applying the DSA numerical procedure. The results should be comparable to those obtained by TS as both the experimental technique and the computer decomposition are based on a distribution of single Debye peaks with Arrhenius relaxation times. The advantage of the DSA is that there is no need of any further assumption on the shape of the decay of the current peak and that each of the elementary peaks obtained can be analyzed with the BFG method in their whole temperature range and not only in a small temperature interval as before. The numerical decomposition results (E_{ai} , τ_{0i} , and P_{0i}) obtained from the global α mode are shown in Fig. 6; in Fig. 6(a) both the experimental trace and the fitted one are drawn. The energy histogram drawn in Fig. 6(b) represents the contribution to the total polarization of each elementary peak as a function of the

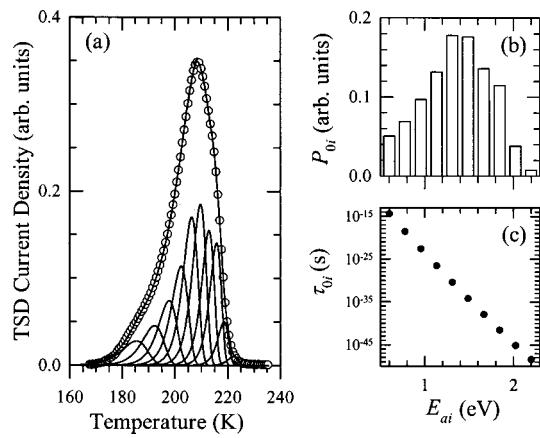


FIG. 6. DSA results for the α relaxation of PCL with Arrhenius relaxation times: (a) experimental points (open circles) and fitted profile (continuous line). The curve is normalized to give a unit polarization. Each elementary process resulting from the best values of E_{ai} , τ_{0i} , and P_{0i} is simulated. (b) Energy histogram showing the contribution to the total polarization of each Debye peak, P_{0i} . (c) Variation of the pre-exponential factor τ_{0i} with the energy bin value.

reorientation energy, E_{ai} ; Fig. 6(c) shows the pre-exponential factors resulting from the fitting for each of the ten energy bins used for this decomposition. It is worth noting that the positions of the peaks in the temperature domain is not imposed here. The extremely low values obtained for τ_{0i} with the TS technique are confirmed here, and consequently, the E_{ai} values are high. The variation range of these two relaxation parameters have been very often qualified as unrealistic. The activation energies and pre-exponential factors determined with the DSA procedure are included as filled triangles in the compensation semi-log plot drawn in Fig. 5 (right-hand side vertical axis) and it is readily seen the agreement between the points obtained by both procedures. The coordinates of the compensation point C' after the DSA decomposition are $\tau_c = (0.008 \pm 0.004)$ s, $T_c = (234 \pm 2)$ K, to be compared with the compensation parameters given for the TS results. In Fig. 7, the relaxation time variation as a function of $1/T$ is represented for each elementary DSA peak; τ_i is calculated with the BFG area method without any approximation and the data represented here covers the values gathered on the whole temperature interval for each pure Debye peak where the peak exists with significant ordinate values, i.e., five decades to be compared with the two decades useable for the TS peaks. The compensation point found is plotted in Fig. 7. The lines which are extrapolated from the linear fit of the points calculated by the DSA procedure, define a convergence region similar to that obtained in the TS case. Figure 5 deserves additional comments as the compensation behavior is a controversial issue when looking for its justification. Independent of the existence of a sound physical interpretation, the fact that the results of the TS and the DSA compare well show their equivalence within experiment errors. Sauer and Moura-Ramos¹⁶ showed, with TS experimental peaks and simulated curves in the same energy and temperature ranges, the appearance of compensation behaviors with different τ_c and T_c , for almost any increase in E_{ai} as one approaches T_g . In conclusion, compensation is

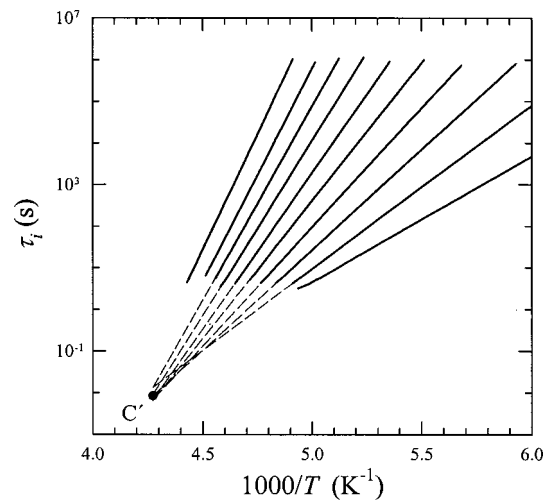


FIG. 7. Relaxation plot $\tau_i(1/T)$ for the α relaxation of PCL obtained from numerical decomposition with the DSA procedure (Arrhenius relaxation times). The compensation point, C' , is obtained from the plot in Fig. 5, $\tau_c = 0.009$ s and $T_c = 234$ K from DSA results only. The continuous lines correspond to the results within the temperature range where each elementary peak is visible. The dashed lines are extrapolations of the continuous ones.

retrieved over a five decades variation when using the numerical decomposition procedure, and the detailed comparison of the TS and DSA shows similar results with Arrhenius relaxation times. This similarity only validates the assumptions and approximations usually made in the analysis of the TS peaks.

An alternative analysis of the global TSDC peak can be attempted when dealing with the cooperative α relaxation where it has very often been reported that the relaxation plots present a curved trace. The application to the α mode of the Eyring, or Arrhenius model established for activated states is dubious since the cooperative character of this relaxation results in a large number of potential barriers, wells, and saddles with varying heights and shapes. The dynamic glass transition has a thermokinetic structure attributed to a degree of disorder in this energy landscape.²⁵ In order to minimize the contribution of the lowest temperature components whose behaviors are best described by Arrhenius temperature dependences, the α peak has been discharged up to a temperature $T_{m\alpha} \sim 10$ K. Additionally, the use of a “clean” peak presents the advantage of minimizing the components whose contributions are more sensitive to the aging of the sample, their maxima being located at temperatures just below T_g . The SADS fitting is used to decompose the “clean” TSDC curve in elementary VTF peaks and the results of the fitting are presented in Fig. 8(a) for the experimental points (open symbols) and the results of the fitting (line). The distribution of VTF energies represented in Figs. 8(b) is much narrower than that obtained with Arrhenius relaxation times and the VTF energy, E'_i ranges between 0.05 and 0.22 eV and $T_0 = 157.5$ K. Also, the pre-exponential VTF factors, τ'_{0i} , resulting from the best fit are plotted in Fig. 8(c) with the corresponding E'_i , staying within reasonable limits as opposed to those reported in Fig. 6(c) when Arrhenius relaxation times were used. Compensation, as visualized in the

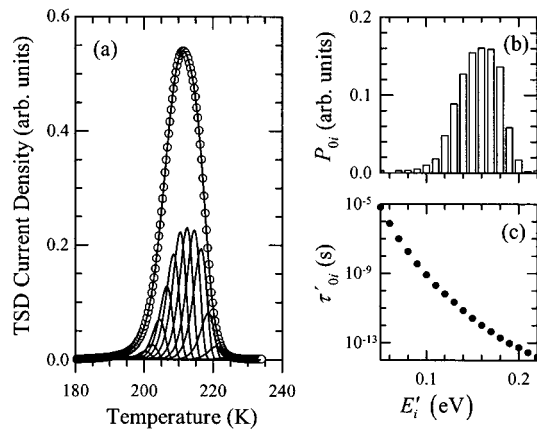


FIG. 8. SADSAs results for the clean α relaxation of PCL with VTF relaxation times: (a) experimental points (open circles) and fitted profile (continuous line). The curve is normalized to give a unit polarization. Each elementary process resulting from the best values of E'_i , τ'_{0i} , $T_0 = 157.5$ K, and P_{0i} is simulated. (b) Energy histogram showing the contribution to the total polarization of each elementary peak, P_{0i} . (c) Variation of the pre-exponential factor τ'_{0i} with the energy bin value, E'_i .

Arrhenius relaxation times formalism, does not hold here as is seen in Fig. 8(c) where a linear relationship between $\log(\tau'_{0i})$ vs E'_i , is not observed. In this way, the decomposition in Debye processes with VTF relaxation times is the correct procedure to analyze an α global peak which has been partially discharged. In this case, compensation does not appear. The misuse of Arrhenius relaxation times to describe cooperative processes seems to be associated to the observation of compensation behavior. The value found for the VTF relaxation time with the SADSAs procedure at the temperature of the peak maximum, $\tau'(T_m)$, allows the calculation of the fragility index introduced by Böhmer *et al.*²⁶ which can be written as

$$m = \frac{E'/kT_g}{\ln(10)(1 - T_0/T_g)^2}, \quad (13)$$

if the strength parameter D is expressed in terms of the VTF energy labeled here as E' , $D = E'/kT_0$. A value of 50 is found which is in excellent agreement with the m value deduced from dielectric spectroscopy performed in a wide range of frequencies and temperatures on this same material.²⁷ Recently, Correia *et al.*²⁸ have found significant curvature in the $\log \tau(1/T)$ plots whose existence is attributed to the polarization of a wide variety of modes in the glass transition region in spite of the restricted amplitude of the polarization window. They use two fragility indexes which do not require VTF dependences and are related to the apparent activation Arrhenius energies found for the most intense TS peak with or without subtracting the zero-entropy enthalpy defined by Eq. (10).

$$m_2 = \Delta H^*(T_m)/\ln(10)kT_m. \quad (14)$$

In our case, this fragility index would be 35 from the most intense TS peak and 33 for the DSA result, which again proves the agreement between TS and our numerical decomposition. The difference is the extent of the temperature range over which the analysis is carried out. Care should be

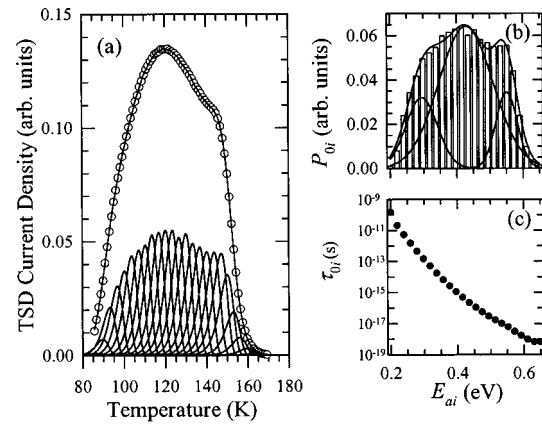


FIG. 9. DSA results for the secondary relaxations of PCL with Arrhenius relaxation times: (a) experimental points (open circles) and fitted profile (continuous line). The curve is normalized to give a unit polarization. Each elementary process resulting from the best values of E_{ai} , τ_{0i} , and P_{0i} is simulated. (b) Energy histogram showing the contribution to the total polarization of each Debye peak, P_{0i} . (c) Variation of the pre-exponential factor τ_{0i} with the energy bin value.

taken as to the significance given to the Arrhenius parameters in the glass transition region which are to be seen as apparent activation energies only and the pre-exponential factor can not be interpreted as an inverse attempt frequency factor.

The TSDC spectrum of PCL drawn in Fig. 2 shows, at low temperature, the broad mode labeled γ and β relaxations which has also been numerically decomposed in elementary peaks with Arrhenius relaxation times. The decomposition into 24 Debye peaks is justified by the wide temperature interval (80 K) covered by this band and the results are presented in Figs. 9(a)–9(c). The energy bins range from 0.20 to 0.65 eV, leading to a variation in pre-exponential factors $10^{-18} < \tau_{0i} < 10^{-10}$ s. The fitting of the energy histogram shown in Fig. 9(b) needs at least three distributed modes. The M pairs of τ_{0i} and E_{ai} found for the best fit of the experimental curve are represented in Fig. 9(c) and no linear relationship is observed between $\log(\tau_{0i})$ and E_{ai} . Nevertheless, compensation effects in secondary relaxations have been found in many cases in previous works on polychlorotrifluoroethylene,³ epoxy–resin glasses,²⁴ polyether block amide,¹⁰ polyethylene terephthalate (PET),²⁹ polyarylates, polysulfone, phenoxy, polyvinylchloride, and polycarbonate.³⁰

An alternative approach has been developed by Starkweather¹⁵ to distinguish among simple modes whose activation entropies are almost zero and which origins are localized motions of dipolar segments, and complex ones with a pronounced cooperative character, whose entropies diverge from the zero-entropy line; these facts are easily observed on a $E_{ai} = f(T_{mi})$ plot. The continuous line drawn in Fig. 10 from the numerical solutions of Eq. (10) represents the zero-entropy line for a constant heating rate of $b = 0.07$ Ks⁻¹ which is the important parameter in the TSDC experiment. The temperature dependence of the activation energies is plotted in Fig. 10 for the decomposition of the α mode by TS (filled circles) and DSA (empty triangles). The results of the numerical decomposition for the secondary relaxation detailed in Fig. 9 are also plotted as open triangles on this

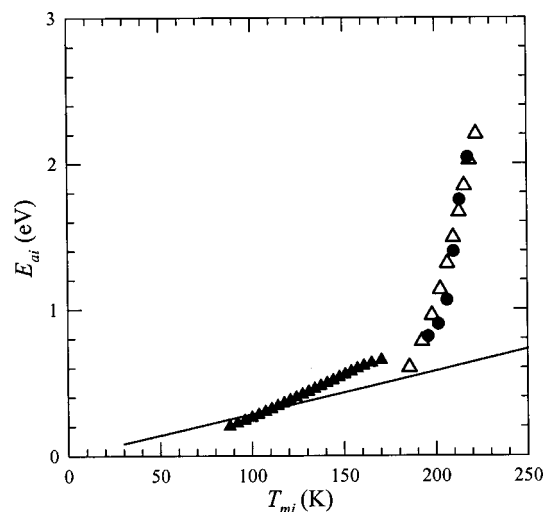


FIG. 10. Starkweather representation of E_{ai} vs T_{mi} in PCL from: ● thermal sampling experiments on the α relaxation; Δ DSA results from the numerical decomposition with Arrhenius relaxation times of the α relaxation; ▲ DSA results from the numerical decomposition of the secondary relaxations.

graph. The points representing the γ relaxation lie next to the zero-entropy line; they are, according to Starkweather model, localized motions with no correlations involved. As the temperature increases, the β relaxation seems to be originated by motions with a small but increasing cooperative character. The presence of a cooperative character in the secondary relaxation of PET has also been proposed to explain the departure from the zero-entropy line of the highest temperature components of the secondary relaxation.²⁹

The escape from the zero-entropy line becomes really significant when one reaches the primary relaxation region, and again the TS and DSA results agree extremely well when the Starkweather criterion is applied to PCL. In the case of PCBA, the results from the analysis of the “clean” α relaxation in PCBA diverge and reach values up to 6.7 eV which are not acceptable. It is worth noting that interpreting the amplitude of the departure from the zero-entropy line as due to the topology of the activation barriers landscape does not agree with the accepted fact that the primary relaxation is not a simply activated process. Even if the points considered were only those corresponding to the rise of the global peak, that is $T_{mi} < T_g$, these points are the most sensitive to the aging that occurs just below the glass transition temperature. If one attributes the departure observed to a cooperative character of the process, the steeply increasing activation entropy of the Eyring process is taken as the manifestation of compensation. This activation entropy is not related to the configurational entropy introduced by Adam and Gibbs²⁰ which can be expressed as the logarithm of the number of configurations corresponding to the average potential energy and volume of the system. This configuration entropy depends on the size of the subsystem and increases monotonically for a given temperature and pressure. Cleaning the α peak to minimize the influence of the Arrhenius contributions and analyzing it with VTF relaxation times seems to be a more reasonable approach than calculating the Eyring parameters ΔH_i^* and ΔS_i^* for a process that is not simply

activated. Moreover, this approach is justified by the excellent agreement shown between the numerical values found for the VTF parameters with those resulting from broadband dielectric spectroscopy experiments on the same samples at frequencies much higher than the equivalent frequency of a TSDC experiment. The variation of the relaxation time with the reciprocal temperature is clearly VTF as the temperature of the maxima of the loss peaks at these frequencies are located well above T_g (see Fig. 9 in Ref. 27).

V. CONCLUSIONS

The detailed comparison of the experimental decomposition of a TSDC global relaxation by using the TS technique and the numerical decomposition obtained with the DSA procedure shows that the results agree well when using Arrhenius relaxation times, in spite of the unreal values for the relaxation parameters given by both methods. The numerical procedures are more rigorous as no approximations are made on the high temperature tail of each of the elementary peaks, the DSA contributions being purely Debye. The linear variation of $\log(\tau_i)$ vs $1/T$ deduced from the BFG method covers five decades and takes into account the whole profile of each Debye peak (τ_{0i} , E_{ai} , and P_{0i}) obtained from the numerical decompositions. The sum of these Debye modes generates the experimental global TSDC α relaxation. The goodness of the fit is characterized by a value in the range of 10^{-9} for the sum of squares residuals between the experimental and fitted points for a unit frozen in polarization. The agreement found between the two methods shows that the approximations made in the TS analysis are appropriate and compensate the uncertainties and assumptions inherent to the analysis of the experimental curve. As for the study of the departure of the activation energies from the zero-entropy line, proposed by Starkweather,¹⁵ TS and DSA results agree very well.

Our approach of decomposing the “clean” segmental mode in Debye peaks with VTF relaxation times is favored by the reasonable values deduced from this analysis for E_i' , τ_{0i}' , and P_{0i} and the fragility index m , in excellent agreement with those deduced from isothermal broadband dielectric spectroscopy experiments performed on the same samples.²⁷ The use of VTF relaxation times for $T \geq T_g$ is justified by the various models^{19,20} which explain the sluggishness of the relaxation times when the glass transition is approached from high temperatures. The use of Arrhenius relaxation times in the DSA numerical decomposition was attempted in order to be able to compare its results to the TS procedure carried on by many research groups. In this framework both methods gave comparable results, thus validating the approximations made in the TS analysis. This validation does not include the compensation behavior that appears in both methods and which is believed to be mainly due to the huge variations of the Arrhenius relaxation parameters as the cooperativity becomes significant in the molecular segmental motion. The partial discharge of the low temperature tail performed on the global peak when fitting it with VTF Debye peaks also helps in minimizing the aging effects which could seriously affect the TS experiments.

- ¹G. Teyssèdre, P. Demont, and C. Lacabanne, *J. Appl. Phys.* **79**, 9258 (1996).
- ²B. B. Sauer, P. Avakian, and H. W. Starkweather, Jr., *J. Polym. Sci., Part B: Polym. Phys.* **34**, 517 (1996).
- ³H. Shimizu and K. Nakayama, *Jpn. J. Appl. Phys., Part 2* **28**, L1616 (1989).
- ⁴M. C. Hernandez, E. Laredo, M. Grimau, and A. Bello, *Polymer* **41**, 7223 (2000).
- ⁵G. Teyssèdre and C. Lacabanne, *J. Phys. D* **28**, 1478 (1995).
- ⁶M. Aldana, E. Laredo, A. Bello, and N. Suarez, *J. Polym. Sci., Part B: Polym. Phys.* **32**, 2197 (1994).
- ⁷A. Bello, E. Laredo, and N. Suarez, in *Proceedings of Conference on Electrical Insulation and Dielectric Phenomena* (IEEE, New York, 1995), p. 440, No. 95 CH35842.
- ⁸C. Bucci, R. Fieschi, and G. Guidi, *Phys. Rev.* **148**, 816 (1966).
- ⁹J. J. Moura Ramos, J. F. Mano, and B. B. Sauer, *Polymer* **38**, 1081 (1997).
- ¹⁰H. S. Faruque and C. Lacabanne, *Polymer* **27**, 527 (1986).
- ¹¹E. Dargent, M. Kattan, C. Cabot, P. Lebaudy, J. Ledru, and J. Grenet, *J. Appl. Polym. Sci.* **74**, 2716 (1999).
- ¹²M. Zielinski, T. Swiderski, and M. Kryszewski, *Polymer* **19**, 883 (1978).
- ¹³C. J. Dias and J. N. Marat-Mendes, in *Proceedings of Tenth International Symposium on Electrets* (IEEE, New York, 1999), p. 371, No. 99 CH36256.
- ¹⁴A. Alegría, L. Goitlandia, and J. Colmenero, *J. Polym. Sci., Part B: Polym. Phys.* **38**, 2105 (2000).
- ¹⁵H. W. Starkweather, Jr., *Macromolecules* **21**, 1798 (1988).
- ¹⁶B. B. Sauer and J. J. Moura Ramos, *Polymer* **38**, 4065 (1997).
- ¹⁷H. J. Eyring, *J. Chem. Phys.* **4**, 283 (1944).
- ¹⁸A. Schönhal, in *Dielectric Spectroscopy of Polymeric Materials*, edited by J. P. Runt and J. J. Fitzgerald (American Chemical Society, Washington, 1997), p. 81.
- ¹⁹M. H. Cohen and D. Turnbull, *J. Chem. Phys.* **31**, 1164 (1959).
- ²⁰G. Adam and J. H. Gibbs, *J. Chem. Phys.* **43**, 139 (1965).
- ²¹E. Laredo, M. Grimau, A. Müller, A. Bello, and N. Suarez, *J. Polym. Sci., Part B: Polym. Phys.* **34**, 2863 (1996).
- ²²A. Bello, E. Laredo, and M. Grimau, *Phys. Rev. B* **60**, 12764 (2000).
- ²³C. Alvares, N. T. Correia, J. J. Moura-Ramos, and A. C. Fernandes, *Polymer* **41**, 2907 (2000).
- ²⁴A. Dufresne and C. Lacabanne, *Polymer* **34**, 3173 (1993).
- ²⁵E. J. Donth, *Relaxations and Thermodynamics in Polymers* (Akademie Verlag GmbH, Berlin, 1992), p. 110.
- ²⁶R. Böhmer, K. L. Ngai, C. A. Angell, and D. J. Plazek, *J. Chem. Phys.* **99**, 4201 (1993).
- ²⁷M. Grimau, E. Laredo, M. C. Perez Y., and A. Bello, *J. Chem. Phys.* **114**, 6417 (2001).
- ²⁸N. T. Correia, C. Alvarez, J. Moura Ramos, and M. Descamps, *J. Chem. Phys.* **113**, 3204 (2000).
- ²⁹J. Menegotto, P. Demont, A. Bernès, and C. Lacabanne, *J. Polym. Sci., Part B: Polym. Phys.* **37**, 3494 (1999).
- ³⁰J. Colmenero, A. Alegría, J. M. Alberdi, J. J. del Val, and G. Ucar, *Phys. Rev. B* **35**, 3995 (1987).